



Title	Development of microfabricated TiO <sub>2</sub> channel waveguides
Author(s)	Furuhashi, Masayuki; Fujiwara, Masazumi; Ohshiro, Takahito; Tsutsui, Makusu; Matsubara, Kazuki; Taniguchi, Masateru; Takeuchi, Shigeki; Kawai, Tomoji
Citation	AIP Advances, 1(3), 032102 <a href="https://doi.org/10.1063/1.3615716">https://doi.org/10.1063/1.3615716</a>
Issue Date	2011-09
Doc URL	<a href="http://hdl.handle.net/2115/49857">http://hdl.handle.net/2115/49857</a>
Rights(URL)	<a href="http://creativecommons.org/licenses/by/3.0/">http://creativecommons.org/licenses/by/3.0/</a>
Type	article
File Information	AIPA1-3_032102.pdf



[Instructions for use](#)

## Development of microfabricated TiO<sub>2</sub> channel waveguides

Masayuki Furuhashi, Masazumi Fujiwara, Takahito Ohshiro, Makusu Tsutsui, Kazuki Matsubara et al.

Citation: *AIP Advances* **1**, 032102 (2011); doi: 10.1063/1.3615716

View online: <http://dx.doi.org/10.1063/1.3615716>

View Table of Contents: <http://aipadvances.aip.org/resource/1/AAIDBI/v1/i3>

Published by the [American Institute of Physics](#).

---

### Related Articles

Silicon nanomembrane based photonic crystal waveguide array for wavelength-tunable true-time-delay lines  
*Appl. Phys. Lett.* **101**, 051101 (2012)

Demonstration of low-loss on-chip integrated plasmonic waveguide based on simple fabrication steps on silicon-on-insulator platform  
*Appl. Phys. Lett.* **101**, 041117 (2012)

Complementary metal–oxide–semiconductor compatible high efficiency subwavelength grating couplers for silicon integrated photonics  
*Appl. Phys. Lett.* **101**, 031109 (2012)

Efficient and broadband polarization rotator using horizontal slot waveguide for silicon photonics  
*Appl. Phys. Lett.* **101**, 021105 (2012)

Trapping of surface plasmon waves in graded grating waveguide system  
*Appl. Phys. Lett.* **101**, 013111 (2012)

---

### Additional information on AIP Advances

Journal Homepage: <http://aipadvances.aip.org>

Journal Information: <http://aipadvances.aip.org/about/journal>

Top downloads: [http://aipadvances.aip.org/most\\_downloaded](http://aipadvances.aip.org/most_downloaded)

Information for Authors: <http://aipadvances.aip.org/authors>

## ADVERTISEMENT



AIPAdvances

Now Indexed in Thomson Reuters Databases

Explore AIP's open access journal:

- Rapid publication
- Article-level metrics
- Post-publication rating and commenting

## Development of microfabricated TiO<sub>2</sub> channel waveguides

Masayuki Furuhashi,<sup>1</sup> Masazumi Fujiwara,<sup>1,2</sup> Takahito Ohshiro,<sup>1</sup> Makusu Tsutsui,<sup>1</sup> Kazuki Matsubara,<sup>1</sup> Masateru Taniguchi,<sup>1,a</sup> Shigeki Takeuchi,<sup>1,2</sup> and Tomoji Kawai<sup>1,3,b</sup>

<sup>1</sup>The Institute of Scientific and Industrial Research, Osaka University, Mihogaoka 8-1, Ibaraki, Osaka 567-0047, JAPAN

<sup>2</sup>Research Institute for Electronic Science, Hokkaido University, Kita 20 Nishi 10, Kitaku, Sapporo, Hokkaido 001-0020, JAPAN

<sup>3</sup>Division of Quantum Phases & Devices, Department of Physics, Konkuk University, Seoul 143-701, Republic of Korea

(Received 8 May 2011; accepted 23 June 2011; published online 15 July 2011)

An optical channel waveguide is a key solution to overcome signal propagation delay. For the benefits of miniaturization, development of microfabrication process for waveguides is demanded. TiO<sub>2</sub> is one of the suitable candidates for the microfabricated waveguide because of the high refractive index and the transparency. In the present study, conventional microfabrication processes manufactured TiO<sub>2</sub> channel waveguides with 1–20 μm width on oxidized Si substrates and the propagation loss was measured. The prepared channels successfully guided light of 632.8 nm along linear and Y-branched patterns. The propagation loss for the linear waveguide was 9.7 dB/cm. *Copyright 2011 Author(s). This article is distributed under a Creative Commons Attribution 3.0 Unported License.* [doi:10.1063/1.3615716]

An optical channel waveguide is a key component of optical interconnection among optical and optoelectronic devices, and plays a crucial role to overcome the bottleneck caused by signal propagation delay.<sup>1,2</sup> For the benefits of compact size, high performance, and low power consumption, development of miniaturization technology for optical channel waveguides is an urgent issue. Recently, silica and glass waveguides with diameters of submicrometer scale were developed and showed good light guiding ability.<sup>3–5</sup> Since the miniaturization limit of waveguides is dominated by diffraction limit  $\lambda/2n$  ( $\lambda$ : wavelength,  $n$ : refractive index of the core),<sup>6</sup> waveguides with a high refractive index are highly required for further miniaturization. Titanium dioxide (TiO<sub>2</sub>) is one of the candidates for the microfabricated waveguides because of the high refractive index and good transparency from infrared to visible region. In past two decades, microfabrication processes for TiO<sub>2</sub> channels have been developed by several groups. In detail, laser-beam lithography, nanoimprint, and electron-beam methods fabricated TiO<sub>2</sub> lines on substrates.<sup>7–10</sup> Furthermore, dry etching process with photolithography formed controlled microfabricated TiO<sub>2</sub> patterns.<sup>11</sup> However, there has been no report for the TiO<sub>2</sub> channel waveguide of which the optical property has been evaluated.

In the present study, TiO<sub>2</sub> channel waveguides with micrometer-size width are manufactured using conventional microfabrication processes and these optical properties are evaluated. First, the TiO<sub>2</sub> films used in the study are characterized by X-ray diffraction (XRD) and ellipsometry. After the fabrication of the TiO<sub>2</sub> channels, guiding of visible light is observed for linear and Y-branched structures. In addition, a propagation loss in linear waveguides is estimated using the cutback technique.

Figure 1 shows the scheme for fabrication of TiO<sub>2</sub> channel waveguides. The substrates were TiO<sub>2</sub> deposited Si wafers, which were purchased from Yamanaka Semiconductor (Japan). The substrates were single-side polished n-type Si(001) wafers (resistivity = 1–20 Ω · cm; thickness =

<sup>a</sup> Author to whom correspondence should be addressed. E-mail: [taniguti@sanken.osaka-u.ac.jp](mailto:taniguti@sanken.osaka-u.ac.jp)

<sup>b</sup> Author to whom correspondence should be addressed. E-mail: [kawai@sanken.osaka-u.ac.jp](mailto:kawai@sanken.osaka-u.ac.jp)



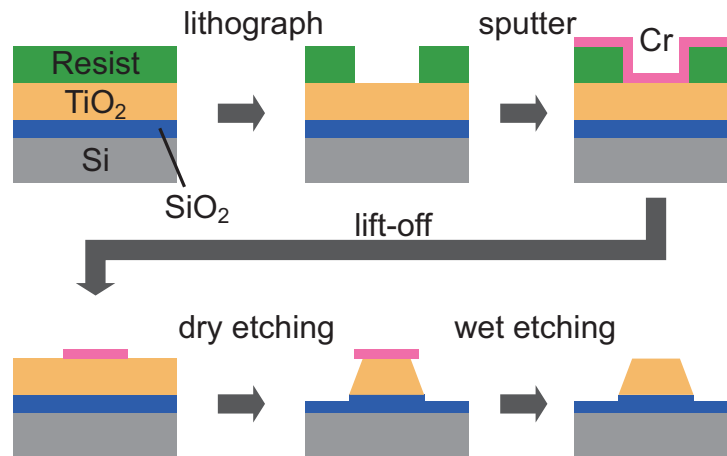


FIG. 1. Fabrication scheme for a TiO<sub>2</sub> channel waveguide on a thermally oxidized Si substrate.

525  $\mu\text{m}$ ), on which SiO<sub>2</sub> layers (thickness = 300 nm) were thermally grown. TiO<sub>2</sub> films (thickness = 600 nm) were deposited by RF magnetron sputtering for a TiO<sub>2</sub> target with Ar/O<sub>2</sub> gas (95 : 5, v/v) at 80 °C on the SiO<sub>2</sub> layers. Characterization of the TiO<sub>2</sub> films were carried out by ellipsometry and XRD method using a spectroscopic ellipsometer UVISEL NIR (Horiba Ltd., Japan) and an X-ray diffractometer X'Pert PRO MRD (PANalytical B. V., Netherland) with Cu K $\alpha$ , respectively. First, the wafer was cut into 20 mm  $\times$  20 mm and 20 mm  $\times$  40 mm for Y-branched and linear waveguides, respectively. Photoresist TSMR-V50 (Tokyo Ohka Kogyo Co., Ltd, Japan) was spin-coated on the pieces of wafer. After the photoresist was exposed for the patterns with 1–20  $\mu\text{m}$  width and developed, Cr films (35 nm) were deposited on the pieces by RF magnetron sputtering with Ar gas. Cr etching masks were formed by lift-off after immersion in N,N-dimethylformamide for half a day and following ultrasonication for 10 min. After the lift-off process, the pieces were cleaned by ultrasonication in ethanol and acetone for 1 min each. Reactive ion etching with CF<sub>4</sub> and Ar gases formed TiO<sub>2</sub> channel waveguides. Solution of (NH<sub>4</sub>)<sub>2</sub>Ce(NO<sub>3</sub>)<sub>6</sub>, HClO<sub>4</sub>, and deionized water (15 : 5 : 80, w/w) removed the residual Cr masks. Finally the samples were washed by deionized water (resistivity > 18.2 M $\Omega$  · cm) and were dried by N<sub>2</sub> stream.

Incidence of light into the waveguides was achieved using a single-mode optical fiber (mode field diameter = 4.3  $\mu\text{m}$ ) that was attached on a manual stage with three linear adjustable axes. The edge of the fiber was brought close to edges of the cleaved waveguides. Outgoing light from the waveguides was collected by a multi-mode optical fiber (core diameter = 50  $\mu\text{m}$ ) and was detected by a photodiode-type detector DET36A/M (Thorlabs, USA) backed by a current amplifier. Here, the amount of the photocurrent was linearly proportional to the light intensity. The source of incident light was a He-Ne laser (wavelength = 632.8 nm; power = 4 mW). Measurements of propagation losses were carried out using the cutback technique.<sup>12</sup> In order to stabilize the positional relation between the incident optical fiber and the waveguides during the measurements, the single-mode optical fiber was adhered to the edge of the waveguides by optical epoxy resin EPO-TEK 301-2 (Epoxy Technology, Inc., USA). This stabilization contributed to the depression of fluctuation of the coupling efficiency between the optical fiber and the waveguides. The propagation losses were estimated from the dependence of the transmitted light intensity on the length of the waveguides.

Figure 2(a) and 2(b) show an XRD data and a dispersion of the refractive index for a non-patterned TiO<sub>2</sub> film on an oxidized Si(001) substrate, respectively. The XRD pattern has no specific peak in the measured region. The lack of distinguishable diffraction lines reveals that the TiO<sub>2</sub> film has an amorphous phase.<sup>13,14</sup> The refractive index  $n$  monotonically decreases with increase of wavelength in the region; the extinction coefficient  $k$  is nearly zero at the wavelength longer than 400 nm and abruptly increases at less than 400 nm. Similar features were reported for TiO<sub>2</sub> films deposited by sputtering.<sup>15–21</sup> The refractive index at 500 nm in Fig. 2(b) is 2.49, which is in good agreement with a TiO<sub>2</sub> film prepared under a low pressure condition.<sup>13</sup> The high refractive

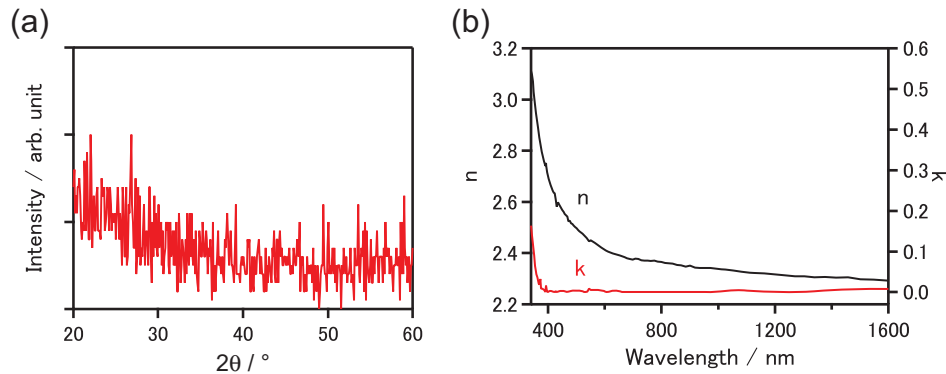


FIG. 2. (a) X-ray diffraction data and (b) refractive index for a non-patterned TiO<sub>2</sub>/SiO<sub>2</sub>/Si sample. Symbols of  $n$  and  $k$  indicate the refractive index and the extinction coefficient, respectively. The small peak and dip structures are artifacts caused by discontinuity of phase in the ellipsometric data.

index ( $n = 2.49$ ) means that the TiO<sub>2</sub> film has a high packing density, since refractive indexes are proportionally related to densities of films.<sup>13,22</sup>

Figure 3(a) and 3(b) show typical scanning electron microscope (SEM) images for a fabricated linear TiO<sub>2</sub> waveguide and its cross section, respectively. The top of the waveguide has a smooth surface. On the contrary, roughness of the sidewalls is large. The outline of the cross section becomes trapezoidal and the morphology of the TiO<sub>2</sub> layer shows a columnar structure. Fig. 3(c) is a top view image of a simple Y-branched waveguide, which diverges from a stem of 25 μm into two 25 μm branches. The angle of two branches is 14°. Roughness of the sidewalls on the branches is larger than that of the stem, because of the 1 μm spatial resolution of the photolithography technique in the present study. Fig. 3(d) shows propagation of red laser light through the Y-branched channel. The incident light from the single-mode optical fiber entered into the stem (left side of the figure) and propagated to the branches (right side). The light clearly divides into two moieties at the Y-junction and the excess loss is 5–6 dB compared with a linear waveguide. This result indicates that the TiO<sub>2</sub> channel has a good guiding ability. Fig. 3(e) shows attenuation of red light in a linear waveguide with 10 μm width. The experimental data were fitted with the following function (Lambert's law):

$$I = I_0 10^{-A(d_0-d)/10}, \quad (1)$$

where  $I$  is the intensity of transmitted light,  $A$  is the propagation loss,  $d_0$  is the initial waveguide length, and  $d$  is the cutback length.  $I_0$  is the initial light intensity, which is treated as a fitting parameter here. In the present study, the amount of the photocurrent is used instead of the light intensity because there is no influence on the estimation of  $A$ . The fitting result by eq. (1) gives a propagation loss  $A = 9.7 \pm 0.4$  dB/cm as an average of three samples.

A propagation loss for a channel waveguide consists of three components; excess absorption of light by defect centers in material, scattering at grain boundaries, and scattering by surface roughness. The former two are caused by imperfection of the TiO<sub>2</sub> film and the latter originates from the device fabrication. Influence of each component on the present propagation loss (9.7 dB/cm) is discussed here. The absorption is strongly related to the crystallinity. As crystal grows, a transmittance edge of a TiO<sub>2</sub> film shifts to a shorter wavelength and the absorption decreases.<sup>23</sup> Since the present TiO<sub>2</sub> film has an amorphous phase, the absorption would be larger than those of properly cured TiO<sub>2</sub> films. The scattering at grain boundaries comes from a microstructure of films. As seen in Fig. 3(b), the cross section of the waveguide shows small columnar grains of TiO<sub>2</sub>. The dependence of extinction coefficients on sputtering conditions elucidated that the scattering loss increased in the case of inhomogeneous and dense TiO<sub>2</sub> films.<sup>13</sup> The scattering by surface roughness depends on the conditions of the fabrication processes and the propagation mode. In the present study, typical sidewall roughness is 50–100 nm; the roughness is suppressed by improvement of the process conditions. The present TiO<sub>2</sub> channel of 10 μm width is a multimode waveguide, which has been

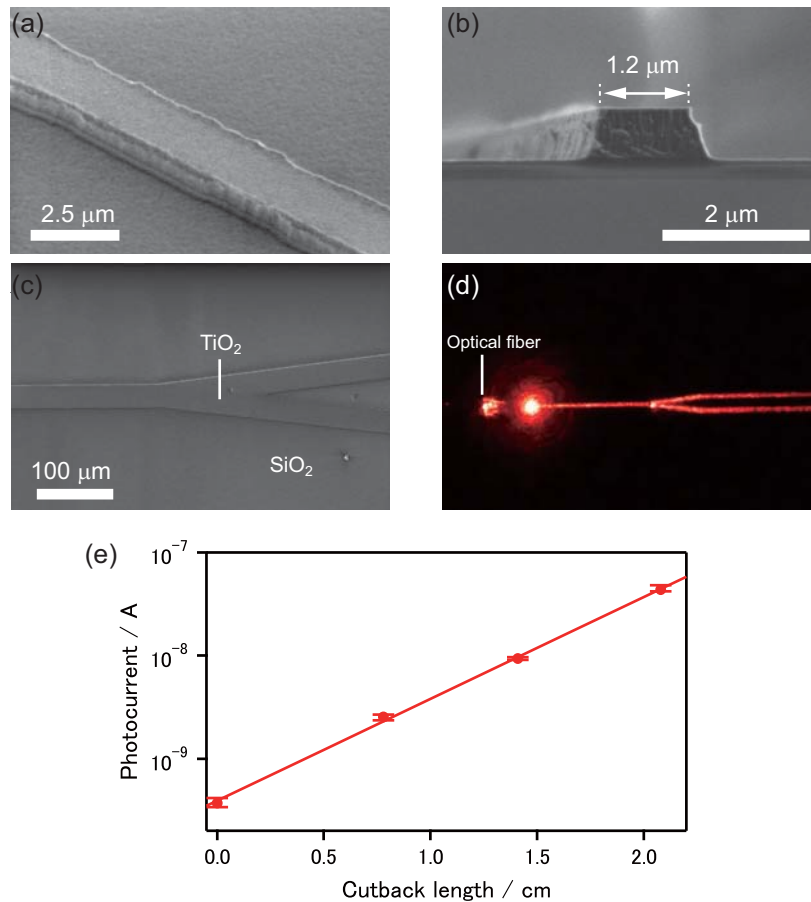


FIG. 3. Scanning electron microscope (SEM) images of (a) bird's eye view and (b) cross sectional view of a linear waveguide. Top view images of SEM and photography for a Y-branched waveguide are shown in (c) and (d), respectively. Typical variation of outgoing light in intensity is shown in (e) as a function of cut length. The result of eq. (1) in the text is shown by the solid line.

estimated from a numerical calculation for a  $\text{TiO}_2$  core with a cross section of  $600 \text{ nm} \times 600 \text{ nm}$  using FIMMWAVE software (Photon Design Ltd., UK). The incident light couples with multiple modes in both horizontal and vertical directions during propagation. Since the coupled higher-order modes have strong distributions in intensity at the interface between a core and a cladding, the higher-order modes are sensitive to surface roughness and rapidly attenuate. However, considering the loss by surface roughness for an Si channel waveguide,<sup>24</sup> contribution of the surface scattering is not ignorable but small for the waveguide of  $10 \text{ }\mu\text{m}$  width. Therefore, the present loss would be mainly due to the imperfection of the  $\text{TiO}_2$  film.  $\text{TiO}_2$  channel waveguides with a high transparency would be obtainable by consideration of following points: crystallinity, surface roughness, film density, film microstructure, and propagation modes. Propagation loss for a  $\text{TiO}_2$  channel waveguide would decrease to those of the planar waveguides ( $2 \text{ dB/cm}$ ), in which the prepared  $\text{TiO}_2$  films are homogeneous, sparse, and thin.<sup>25,26</sup>

In summary,  $\text{TiO}_2$  channel waveguides with micrometer-size width were fabricated using microfabrication process and their optical characteristics were observed. The channels successfully guided light of  $632.8 \text{ nm}$  along linear and Y-branched patterns. The estimated propagation loss revealed that the  $\text{TiO}_2$  channel waveguides had less transparency than those of past planar waveguides. The authors gave the strategy for the fabrication of highly transparent  $\text{TiO}_2$  channel waveguides. The present study contributes to development of miniaturization technology for optical interconnection.

## ACKNOWLEDGEMENTS

The authors would like to thank Mr. Masato Tanida for his technical assistance. This research was supported by the Funding Program for World-Leading Innovative Research and Development on Science and Technology “Innovative NanoBiodevice based on Single Molecule Analysis” from the Japan Society for the Promotion of Science. Takeuchi and Fujiwara acknowledge the supports from the Management Expenses Grants for National Universities Corporations from MEXT and a Grant-in-Aid from the Japan Society for the Promotion of Science.

- <sup>1</sup> L. C. Kimerling, *Appl. Surf. Sci.* **159-160**, 8 (2000).
- <sup>2</sup> M. Haurylau, C. Guoqing, C. Hui, Z. Jidong, N. A. Nelson, D. H. Albonesi, E. G. Friedman and P. M. Fauchet, *IEEE J. Sel. Top. Quantum Electron.* **12**, 1699 (2006).
- <sup>3</sup> L. Tong, R. R. Gattass, J. B. Ashcom, S. He, J. Lou, M. Shen, I. Maxwell and E. Mazur, *Nature* **426**, 816 (2003).
- <sup>4</sup> L. Tong, J. Lou, R. R. Gattass, S. He, X. Chen, Liu and E. Mazur, *Nano Lett.* **5**, 259 (2005).
- <sup>5</sup> L. Tong and E. Mazur, *J. Non-Cryst. Solids* **354**, 1240 (2008).
- <sup>6</sup> J. Takahara, S. Yamagishi, H. Taki, A. Morimoto and T. Kobayashi, *Opt. Lett.* **22**, 475 (1997).
- <sup>7</sup> M. Haruna, Y. Murata and H. Nishihara, *Jpn. J. Appl. Phys., Part 1* **31**, 1593 (1992).
- <sup>8</sup> K. S. Park, E. K. Seo, Y. R. Do, K. Kim and M. M. Sung, *J. Am. Chem. Soc.* **128**, 858 (2005).
- <sup>9</sup> B. Liu and S.-T. Ho, *J. Electrochem. Soc.* **155**, P57 (2008).
- <sup>10</sup> K.-m. Yoon, K.-Y. Yang, H. Lee and H.-S. Kim, *J. Vac. Sci. Technol. B* **27**, 2810 (2009).
- <sup>11</sup> S. Norasetthekul, P. Y. Park, K. H. Baik, K. P. Lee, J. H. Shin, B. S. Jeong, V. Shishodia, E. S. Lambers, D. P. Norton and S. J. Pearton, *Appl. Surf. Sci.* **185**, 27 (2001).
- <sup>12</sup> A. Bornstein, N. Croitoru and E. Marom, *J. Non-Cryst. Solids* **74**, 57 (1985).
- <sup>13</sup> L.-J. Meng and M. P. dos Santos, *Thin Solid Films* **226**, 22 (1993).
- <sup>14</sup> C. K. Chung, M. W. Liao and C. W. Lai, *Thin Solid Films* **518**, 1415 (2009).
- <sup>15</sup> A. Karuppasamy and A. Subrahmanyam, *J. Appl. Phys.* **101**, 064318 (2007).
- <sup>16</sup> D. Mardare and P. Hones, *Mater. Sci. Eng., B* **68**, 42 (1999).
- <sup>17</sup> L.-J. Meng, V. Teixeira, H. N. Cui, F. Placido, Z. Xu and M. P. dos Santos, *Appl. Surf. Sci.* **252**, 7970 (2006).
- <sup>18</sup> V. Straňák, M. Čada, M. Quaas, S. Block, R. Bogdanowicz, Š. Kment, H. Wulff, Z. Hubička, C. A. Helm, M. Tichý and R. Hippler, *J. Phys. D: Appl. Phys.* **42**, 105204 (2009).
- <sup>19</sup> S. Tanemura, L. Miao, P. Jin, K. Kaneko, A. Terai and N. Nabatova-Gabain, *Appl. Surf. Sci.* **212-213**, 654 (2003).
- <sup>20</sup> M. H. Suhail, G. M. Rao and S. Mohan, *J. Appl. Phys.* **71**, 1421 (1992).
- <sup>21</sup> H. Xie, F. L. Ng and X. T. Zeng, *Thin Solid Films* **517**, 5066 (2009).
- <sup>22</sup> D. Mergel, D. Buschendorf, S. Eggert, R. Grammes and B. Samset, *Thin Solid Films* **371**, 218 (2000).
- <sup>23</sup> W.-H. Wang and S. Chao, *Opt. Lett.* **23**, 1417 (1998).
- <sup>24</sup> K. K. Lee, D. R. Lim, H.-C. Luan, A. Agarwal, J. Foresi and L. C. Kimerling, *Appl. Phys. Lett.* **77**, 1617 (2000).
- <sup>25</sup> R. Mechiakh, F. Mérieux, R. Kremer, R. Bensaha, B. Boudine and A. Boudrioua, *Optical Materials* **30**, 645 (2007).
- <sup>26</sup> T. Alasaarela, T. Saastamoinen, J. Hiltunen, A. Säynätjoki, A. Tervonen, P. Stenberg, M. Kuittinen and S. Honkanen, *Appl. Opt.* **49**, 4321 (2010).